High-fidelity one-qubit operations under random telegraph noise

Mikko Möttönen,[1,2,*] Rogerio de Sousa,[1] Jun Zhang,[1] and K. Birgitta Whaley[1]
[1]*Department of Chemistry and Pitzer Center for Theoretical Chemistry, University of California, Berkeley, California 94720, USA*
[2]*Laboratory of Physics, Helsinki University of Technology, P.O. Box 4100, FIN-02015 HUT, Finland*
(Received 5 August 2005; revised manuscript received 30 November 2005; published 17 February 2006)

We address the problem of implementing high-fidelity one-qubit operations subject to time-dependent noise in the qubit energy splitting. We show with explicit numerical results that high-fidelity bit flip operations may be generated by imposing bounded control fields. For noise correlation times shorter than the time for a π pulse, the time-optimal π pulse itself yields the highest fidelity. For very long correlation times, fidelity loss is approximately due to systematic error, which is efficiently tackled by compensation for off resonance with a pulse sequence (CORPSE). For intermediate ranges of the noise correlation time, we find that short CORPSE, which is less accurate than CORPSE in correcting systematic errors, yields higher fidelities. Numerical optimization of the pulse sequences using gradient ascent pulse engineering results in noticeable improvement of the fidelity for a bit flip operation on the computational basis states and a small but still positive fidelity enhancement for the NOT gate.

DOI: 10.1103/PhysRevA.73.022332 PACS number(s): 03.67.Pp, 03.67.Lx, 03.65.Yz

I. INTRODUCTION

In physical implementations of quantum computers, one of the most challenging tasks is to find an efficient and experimentally feasible way to overcome the problems caused by undesired interactions between the quantum bits, qubits, and their surrounding environment. These interactions, which destroy the quantum interference between qubit states, lead to errors and loss of fidelity, a phenomenon generally referred to as decoherence.

A variety of methods to fight decoherence have been proposed in the literature. These include error-correcting codes [1,2], decoherence free subspace coding [3,4], noiseless subsystem coding [5], dynamical decoupling [6–8], quantum feedback control [9–11], quantum reservoir engineering [12], numerical design of pulse sequences robust to experimental inhomogeneities [13], and optimal control based on Markovian master equation descriptions [14]. Most of these schemes are not efficient in making full use of all the physical resources, or are restricted in their applicability. For example, encoding schemes employing decoherence free subspaces or error-correcting codes store the quantum information in a specific portion of the whole Hilbert space, or encode several physical qubits into one logical qubit. Design and applicability of such codes depends on the nature of the decoherence sources and imposes additional requirements on encoding and decoding. Dynamical decoupling schemes possess the attractive feature that they require no ancillary qubits, since the interactions between the qubits and the environment are effectively averaged out by applying external control fields. It has also been shown that such decoupling can be realized using finite energy soft pulses [8] and that it is possible to carry out qubit rotations without disturbing the decoupling process [7]. However, dynamical decoupling is based on stroboscopic pulsing of the qubit, at a rate significantly faster than the usual characteristic frequency of environmental fluctuations. This kind of pulsing requires strong control fields, which might be problematic to realize experimentally. For example, it has been pointed out that the high-energy deposition needed for dynamical decoupling of nuclear spins is incompatible with the low-temperature requirement in some qubit implementations [15].

In this paper, we consider the design of fidelity-optimized one-qubit operations in a noisy environment. The errors on a single qubit can be put into two categories, namely, phase and flip errors corresponding to the Pauli matrices σ_z and σ_x in the system Hamiltonian, respectively. The methods we present here are general and applicable to both types of errors, as well as to a combination of the two. To illustrate the approach, we restrict our attention to only the phase errors specified by a stochastic time-varying amplitude. This study is motivated by experiments on superconducting solid-state qubits [16,17] for which random telegraph noise (RTN) [18] in the qubit energy splitting is thought to provide an appropriate phenomenological model for the effect of environmental fluctuations due to a localized defect [19–21]. Whereas an ensemble of RTN fluctuators models the ubiquitous $1/f$ noise in electronic circuits [22], solid-state devices on the nanoscale are often found to be affected by a single RTN source [23,24] that is characterized by its correlation time τ_c. The methods demonstrated here to suppress the errors due to RTN on the qubit energy splitting are also applicable to general one-qubit errors, including systematic errors in the rotation angle [25,26], and can also be extended to multiqubit systems.

Composite pulse sequences are known to provide an efficient way to reduce errors due to time-independent off-resonant perturbations [13,27], e.g., compensation for off-resonance with a pulse sequence (CORPSE) [28,29]. Here we focus on the situation in which the perturbation of a qubit is fluctuating in time and seek to suppress the decoherence arising from this time-dependent noise by imposition of a bounded control field. The typical time scale for qubit manipulation is of the order of $\gtrsim \hbar/a_{\max}$, where $a_{\max}$ is the

*Electronic address: mikko.mottonen@tkk.fi

maximum energy amplitude of the control field. We provide an analysis of coherence control for variable noise correlation times τ_c, ranging from short noise-correlation times satisfying $\tau_c a_{\max}/\hbar \ll 1$ to the long correlation time regime, $\tau_c a_{\max}/\hbar \gg 1$. In the former case, the decoherence is well described by the standard methods based on Markovian master equations [30]. In the limit $\tau_c \to \infty$, the fidelity loss is due to systematic time-independent errors, for which high-fidelity qubit rotations can be achieved using the composite-pulse approach [27–29]. For large but finite values of τ_c, coherent control of the qubit for times much longer than the characteristic time $\hbar/a_{\max}$ can be achieved using dynamical decoupling through the sequential application of control pulses at time intervals much less than τ_c [6]. Consequently, each control pulse must be implemented within an even shorter time scale than the characteristic time $\hbar/a_{\max}$, leading to the condition $\tau_c a_{\max}/\hbar \gg 10-100$ for achieving substantial coherence enhancement by such a decoupling approach. Here we are particularly interested in the intermediate regime given by $\tau_c a_{\max}/\hbar \sim 1$. This regime is important since it is outside the range of validity of both dynamical decoupling and control methods based on Markovian master equations. Moreover, recent experiments probing decoherence of superconducting qubits [16,17] suggest that this regime may be important in some experimental realizations of qubits.

It was stated in Ref. [29] that CORPSE is the shortest sequence in the family of composite pulse sequences correcting systematic errors as efficiently as possible and composed of up to three pulses. Therefore, it was considered to be the most useful one. However, a composite pulse sequence referred to as short CORPSE (SCORPSE) [29] is shorter than CORPSE in time, and hence, it may still be of some interest, depending on the physical scenario. We illustrate this fact here by showing that SCORPSE actually yields higher fidelities than CORPSE in the regime of intermediate noise correlation time, $\tau_c a_{\max}/\hbar \sim 1$, for the one-qubit example studied here. The optimal performance of CORPSE is, in fact, seen to be limited to just the long correlation time limit, $\tau_c \to \infty$. We also go beyond these standard composite pulse sequences to obtain fidelity-optimized pulses consisting of large numbers of pulse amplitudes that are numerically derived using an adaptation of the method of gradient ascent pulse engineering (GRAPE) [31]. We find that in the range $\tau_c a_{\max}/\hbar \sim 1$ such an optimized pulse profile can increase the fidelity of quantum operations by up to 30% in comparison to the standard composite pulse sequences, such as CORPSE and SCORPSE.

The GRAPE algorithm was originally developed for finding control pulses in closed quantum systems [31]. In this paper, we adapt GRAPE to yield fidelity-optimized bounded control pulses in a noisy quantum system. We represent the density matrix as a sum over trajectories of controlled unitary dynamics, in which each trajectory describes the unitary evolution of the system under the same control field but a different sample path of RTN. We refer to this representation as the unitary quantum trajectory approach. The fidelity for a quantum operation is optimized using the gradient method as in the original GRAPE algorithm. We study the fidelity improvements arising from this optimization by analyzing bit flip operations on a single qubit. In particular, the fidelity enhancement for bit flips on the computational basis states is observed to be significant. We define an average fidelity for the one-qubit NOT gate by averaging the fidelity of the bit flip state transformation over all pure initial states, which is appropriate in the absence of specific knowledge about initial conditions for a given application. This average fidelity obtained from GRAPE is also higher than the corresponding values obtained from the standard composite pulse sequences, but to a lesser extent than for the specific instance on the computational basis states. More extensive numerical studies will therefore be useful for determination of fidelity-optimal pulse sequences for specific applications, e.g., algorithms, where input states for the NOT gate are restricted to a subset of the whole Hilbert space.

The remainder of this paper is organized as follows. In Sec. II, we characterize the system Hamiltonian, the noise model, and the fidelity measures employed here. Section III introduces the pulse sequence-generation methods we use for the noisy qubit systems. Section IV presents the results obtained for high-fidelity implementation of two quantum operations. The first is a single quantum state transformation corresponding to bit flips on the computational basis states. The second is the one-qubit NOT gate, which is independent of the state of the qubit. Finally, Sec. V concludes the paper with a discussion of ramifications and possible extensions of this work.

II. SYSTEM CHARACTERIZATION

We consider a single qubit described by the effective Hamiltonian

$$H = \sum_{i \in \{x,y,z\}} \tfrac{1}{2}[a_i(t) + \eta_i(t)]\sigma_i, \tag{1}$$

where the symbols $\{\sigma_i\}$ denote the Pauli spin matrices [32], $\{\eta_i(t)\}$ are the amplitudes of the environmental noise, and $\{a_i(t)\}$ are the external control fields. Note that the latter are parametrized here by their corresponding energy amplitudes, rather than the actual physical control fields, e.g., electric-field amplitudes. We assume that the strength of the control fields is finite and denote their maximum possible value by $a_{\max}$. To simplify the discussion, we consider here only the case where there is no control in the y or z directions and no noise in the x and y directions. Under these assumptions, the Hamiltonian becomes

$$H = \tfrac{1}{2}a(t)\sigma_x + \tfrac{1}{2}\eta(t)\sigma_z, \tag{2}$$

where the control field $a := a_x \in [-a_{\max}, a_{\max}]$ and we have used the notation $\eta(t) := \eta_z(t)$.

For RTN, the amplitude of the noise η changes randomly in time between two values $-\Delta$ and Δ. The quantity Δ describes the strength of the noise, and the frequency of the jumps between values $-\Delta$ and Δ is determined by the correlation time τ_c. Specifically, the probability of the noise to jump in an infinitesimal time interval of length dt is given by dt/τ_c. Hence, the probability of no jumps taking place in a time interval of length t is

$$p_0(t) = e^{-t/\tau_c}. \tag{3}$$

In generating sample trajectories of RTN, Eq. (3) can also be inverted to yield the sojourn time before a jump takes place. Thus, we get a sample trajectory of RTN by taking random numbers $p_i \in (0,1)$ and then, deriving the corresponding jump time instants,

$$t_i = \sum_{j=1}^{i} -\tau_c \ln(p_j). \tag{4}$$

Using the values of these jump times, we can express the noise process $\eta(t)$ as

$$\eta(t) = (-1)^{\Sigma_i \Theta(t-t_i)} \eta(0), \tag{5}$$

where $\Theta(t)$ is the Heaviside step function.

In the limit $\tau_c \to 0$ and $\Delta \to \infty$ such that $\Delta^2 \tau_c/2 \equiv \hbar^2 \Gamma$ remains finite, this RTN model reduces to white noise, i.e., the noise correlation function becomes

$$\langle \eta(t)\eta(t') \rangle = \Delta^2 e^{-2|t-t'|/\tau_c} \tag{6}$$

$$\xrightarrow[\tau_c \to 0]{\Delta \to \infty} \hbar^2 \Gamma \delta(t-t'). \tag{7}$$

In this limit, one may apply the Markovian master equation formalism, which leads to a decoherence time of the order of Γ^{-1} [30]. In this work, we do not apply a master equation approach but instead simulate the RTN numerically and express the density matrix of the system by a unitary quantum trajectory approach that is valid for all values of the correlation time τ_c.

Since we use an effective Hamiltonian operating solely on the qubit rather than treating the full quantum dynamics of both the qubit and the environment, we need to average over different noise trajectories in order to obtain the system dynamics under the influence of RTN. Therefore, the dynamics of the system density matrix ρ can be written as

$$\rho(t) = \lim_{N\to\infty} \frac{1}{N} \sum_{k=1}^{N} U_k \rho_0 U_k^\dagger, \tag{8}$$

where $\rho_0 = \rho(0)$ is the initial state of the system and the operators $\{U_k\}$ refer to unitary time evolution of the system under a certain trajectory $\eta_k(t)$. Formally, the operator U_k is written as

$$U_k = \mathcal{T} e^{-(i/2)\int_0^t d\tau [a(\tau)\sigma_x + \eta_k(\tau)\sigma_z]/\hbar}, \tag{9}$$

where $\mathcal{T}$ is the time-ordering operator.

Let ρ_f be the desired final state of the system. Following Ref. [31], we define a fidelity function for the corresponding state transformation in the presence of noise as

$$\phi = \mathrm{tr}\{\rho_f^\dagger \rho_T\}, \tag{10}$$

where $\rho_T := \rho(T)$ is the actual state of the system at the final time instant T. Substituting Eq. (8) into Eq. (10), we obtain the fidelity for the desired quantum state transformation from ρ_0 to ρ_f as

$$\phi(\rho_f, \rho_0) = \lim_{N\to\infty} \frac{1}{N} \sum_{k=1}^{N} \mathrm{tr}\{\rho_f^\dagger U_k \rho_0 U_k^\dagger\}. \tag{11}$$

Equation (11) shows that this fidelity function can be viewed as an average over fidelity functions corresponding to individual unitary time developments in noiseless quantum systems that are each characterized by different noise-dependent evolution operators $\{U_k\}$.

Equation (11) defines the fidelity for a state transformation between specified initial and final states. However, we also want to obtain a measure of the performance of a quantum gate U_f, i.e., a fidelity function that is independent of the initial state is required. In order to obtain such a fidelity, we choose ρ_0 and ρ_f such that $\rho_f = U_f \rho_0 U_f^\dagger$, and perform averaging over the initial state ρ_0. In general, there may be some nontrivial dependence of the fidelity $\phi(\rho_f, \rho_0)$ on the initial state, which can be utilized for some applications, e.g., algorithms in which the gate U_f is always applied to a specific set of input states. Since we consider here a general formulation of the fidelity for quantum gates without prior knowledge of the states the gate U_f is to be applied, we average over a uniform distribution of initial states ρ_0 on the Bloch sphere. Thus, we parametrize the state ρ_0 as

$$\rho_0 = \frac{(I + c_x\sigma_x + c_y\sigma_y + c_z\sigma_z)}{2}, \tag{12}$$

where c_i are real numbers satisfying $c_1^2 + c_2^2 + c_3^3 = 1$. The gate fidelity function is defined as

$$\Phi(U_f) = \frac{1}{4\pi} \int_{c_x^2+c_y^2+c_z^2=1} d\Omega \, \phi(\rho_f, \rho_0), \tag{13}$$

where $d\Omega$ is an infinitesimal solid angle on the Bloch sphere. Substitution of Eq. (11) into Eq. (13) yields

$$\Phi(U_f) = \frac{1}{2} + \lim_{N\to\infty} \frac{1}{12N} \sum_{k=1}^{N} \sum_{j=1}^{3} \mathrm{tr}\{U_f \sigma_j U_f^\dagger U_k \sigma_j U_k^\dagger\}. \tag{14}$$

The average fidelity $\Phi(U_f)$ for quantum gate optimization may be computed efficiently from Eq. (14) and provides a useful assessment of the gate performance independent of the specifics of any individual application. We note that there may be some input states yielding much lower fidelities than this average, which could be further explored by replacing the average over the initial states ρ_0 in Eq. (13) with a minimization of $\phi(\rho_f, \rho_0)$ with respect to a set of prescribed initial input states or, indeed, with respect to all input states. Such a minimization provides a useful worst-case estimation, i.e., independent of the initial state within a given set, a certain level of fidelity is always achieved. These issues require more intensive computational analysis but will be useful to explore in future work, particularly if specific applications restrict the range of input states. For the purpose of this study, we shall analyze only the gate fidelity obtained from an unbiased average as defined in Eq. (14).

III. PULSE SEQUENCES FOR NOISY SYSTEMS

In this section, we introduce the pulse sequences that will be used for suppression of decoherence. Our reference pulse

sequence is the time-optimal π pulse given by

$$a_\pi(t) = a_{\max}, \quad \text{for } t \in [0, \pi\hbar/a_{\max}]. \tag{15}$$

In the absence of noise, i.e., for $\Delta=0$, the π pulse is the most efficient way of achieving a NOT gate. We consider here the two composite pulse sequences CORPSE and SCORPSE [27–29], which were originally designed to correct systematic errors in the implementation of one-qubit quantum gates. The control field corresponding to the CORPSE pulse sequence is

$$a_C(t) = \begin{cases} a_{\max}, & \text{for } 0 < t' < \dfrac{\pi}{3} \\ -a_{\max}, & \text{for } \pi/3 \leqslant t' \leqslant 2\pi \\ a_{\max}, & \text{for } 2\pi < t' < \dfrac{13\pi}{3}, \end{cases} \tag{16}$$

where the time t is related to the dimensionless time t' by $t'=a_{\max}t/\hbar$. For the SCORPSE pulse sequence, the control field is

$$a_{SC}(t) = \begin{cases} -a_{\max}, & \text{for } 0 < t' < \dfrac{\pi}{3} \\ a_{\max}, & \text{for } \pi/3 \leqslant t' \leqslant 2\pi \\ -a_{\max}, & \text{for } 2\pi < t' < \dfrac{7\pi}{3}. \end{cases} \tag{17}$$

In the absence of noise, the CORPSE and SCORPSE pulse sequences also generate the NOT gate, but their operation time is longer than that of the time-optimal π pulse. To demonstrate the accuracy of CORPSE and SCORPSE in the presence of systematic error, i.e., $\tau_c \to \infty$ implying $\eta(t) \equiv \eta(0)$, we consider a bit flip state transformation, from the south pole to the north pole of the Bloch sphere. For $\eta(t) \equiv \Delta$ in Eq. (2), the fidelities from Eq. (10) are of the form

$$\phi_\pi = 1 - \left(\frac{\Delta}{a_{\max}}\right)^2 + 0.38 \times \left(\frac{\Delta}{a_{\max}}\right)^4 + \mathcal{O}\left(\frac{\Delta}{a_{\max}}\right)^6, \tag{18}$$

$$\phi_C = 1 - 0.0065 \times \left(\frac{\Delta}{a_{\max}}\right)^4 + \mathcal{O}\left(\frac{\Delta}{a_{\max}}\right)^6, \tag{19}$$

$$\phi_{SC} = 1 - 2.7 \times \left(\frac{\Delta}{a_{\max}}\right)^4 + \mathcal{O}\left(\frac{\Delta}{a_{\max}}\right)^6, \tag{20}$$

for the π pulse, CORPSE, and SCORPSE, respectively. Note that the deviation from unity of the π-pulse fidelity is second order in $\Delta/a_{\max}$, in contrast to the deviations for the CORPSE and SCORPSE fidelities, which are only fourth order in $\Delta/a_{\max}$. Moreover, the coefficients of the fourth-order term in the two composite pulse sequences differ by almost a factor of 400, implying that CORPSE is much more efficient than SCORPSE in correcting systematic error.

An alternative to these composite pulse sequences is provided by numerical construction of pulse sequences optimized for maximum fidelity. Such fidelity-optimized sequences may be constructed by an adaptation of the GRAPE algorithm [31], which was originally designed to steer the dynamics of coupled nuclear spins. No noise effects or bounds on control fields are included in the original implementation. For full details of the GRAPE algorithm for closed quantum systems, see Ref. [31].

The key feature of the GRAPE algorithm is to approximate the continuous pulse shape on a time interval $[0,T]$ by a function that is constant on n small time intervals of length $\delta t = T/n$ and then to derive the corresponding gradients of the fidelity function with respect to these constant values. Let U_k^m be the unitary time-evolution operator corresponding to the time interval $[(m-1)\delta t, m\delta t]$ and to the noise trajectory η_k. In this interval, the control field is approximated by a constant a^m. Since the fidelity function $\phi(\rho_f, \rho_0)$ is an average of the fidelity functions used in Ref. [31], the gradient of $\phi(\rho_f, \rho_0)$ is obtained as an average of the gradients derived in Ref. [31]. Thus,

$$\frac{\partial\phi(\rho_f,\rho_0)}{\partial a^m} = -\frac{i\delta t}{2\hbar} \lim_{N\to\infty} \frac{1}{N} \sum_{k=1}^{N} \mathrm{tr}\{(\lambda_k^m)^\dagger [\sigma_x, \rho_k^m]\}, \tag{21}$$

where

$$\lambda_k^m = (U_k^n U_k^{n-1} \cdots U_k^{m+1})^\dagger \rho_f U_k^n U_k^{n-1} \cdots U_k^{m+1} \tag{22}$$

and

$$\rho_k^m = U_k^m U_k^{m-1} \cdots U_k^1 \rho_0 (U_k^m U_k^{m-1} \cdots U_k^1)^\dagger. \tag{23}$$

In the case that there exist other control terms $\{a_k^c(t)H_k^c\}$ in the Hamiltonian, the corresponding gradients can be obtained from Eq. (21) by substituting a by a_k^c and σ_x by $2H_k^c$.

We note that for noise strength $\Delta=0$, all the individual RTN trajectories are identical and, consequently, the averaging and limiting procedures in Eq. (21) can be omitted. In this case, Eq. (21) reduces to the equation for noiseless systems derived in Ref. [31].

To derive the gradient of the average fidelity Φ, we apply the identity

$$\Phi(U_f) = \frac{1}{2} + \frac{1}{12} \sum_{j=1}^{3} \phi(U_f \sigma_j U_f^\dagger, \sigma_j). \tag{24}$$

Hence, the gradient of Eq. (24) can be obtained from Eq. (21) as

$$\frac{\partial\Phi(U_f)}{\partial a^m} = \frac{1}{12} \sum_{j=1}^{3} \frac{\partial\phi(U_f\sigma_j U_f^\dagger, \sigma_j)}{\partial a^m}. \tag{25}$$

In the GRAPE algorithm, we calculate the gradient of the desired fidelity function using Eq. (21) or (25) and update the control fields by moving along the direction of the gradient with the restriction $a \in [-a_{\max}, a_{\max}]$. This procedure results in an optimized pulse sequence for a given operation time T. Moreover, the fidelity is also optimized with respect to the operation time.

We note that the pulse sequences yielding the optimal fidelity for each set of system parameters are not unique. In order to find as smooth and as simple a sequence as possible, we therefore start from a constant control field and use the gradient method to maximize the fidelity. To ascertain whether our solution achieves a local or the global maximum

in fidelity, we repeated the procedure for several different, uncorrelated initial values of the control field. This resulted in different pulse sequences with equal fidelities, suggesting that we have, indeed, found the global maximum, though this cannot be conclusively claimed. Thus, when we refer to the results of the GRAPE algorithm, we shall describe the corresponding pulse sequences as optimized rather than optimal.

IV. HIGH-FIDELITY ONE-QUBIT OPERATIONS

In this section, we present numerical results of the implementation of high-fidelity one-qubit operations, which were obtained using the GRAPE algorithm, and compare the fidelities to those obtained from the π-pulse, CORPSE, and SCORPSE sequences. We restrict out attention to two quantum operations on the one-qubit system, namely, the state transformation corresponding to a bit flip on the computational basis states and the one-qubit NOT gate.

A. Bit flip on computational basis states

We consider the flipping of a one-qubit state from one of the two poles of the Bloch sphere to the other. This is a specific application of the NOT gate to the computational basis states and constitutes a single quantum state transformation. This specific transformation may arise, for example, when some qubits of a multiqubit register need to be flipped to reach a nontrivial state after a collective initialization. The initial and final states are taken as the pure state density matrices

$$\rho_0 = \begin{pmatrix} 0 & 0 \\ 0 & 1 \end{pmatrix} \quad \text{and} \quad \rho_f = \begin{pmatrix} 1 & 0 \\ 0 & 0 \end{pmatrix}. \tag{26}$$

corresponding to the state vectors $|0\rangle$ and $|1\rangle$ at the south and north poles of the Bloch sphere, respectively. We first consider the performance of the reference π pulse, CORPSE, and SCORPSE for a fixed noise strength Δ in two limiting cases: vanishing noise correlation time, and infinite noise correlation time.

Case 1. $\tau_c \to 0$. In this case, RTN averages out due to the well-known phenomenon of motional narrowing [33] since the noise changes its sign so rapidly that there is no time for the qubit to drift into the direction of the noise. Therefore, all composite pulse sequences as well as the reference π pulse will give unit fidelity in this limit and, for practical purposes, the time optimal π pulse will be preferred. Furthermore, as τ_c approaches zero, the time optimal π pulse is expected to have the highest fidelity because of its short operation time.

Case 2. $\tau_c \to \infty$. In this case, RTN reduces to a constant drift. For large but finite τ_c the drift may be treated as approximately constant. In comparison to a π pulse, pulse sequences such as CORPSE and SCORPSE, which are specifically designed to correct time-independent systematic errors will clearly improve the fidelity of the desired quantum operation. The asymptotic fidelities for each of these pulse sequences are given in Eqs. (18)–(20).

In Fig. 1, the fidelities obtained from π-pulse, CORPSE, and SCORPSE pulse sequences for a bit flip are plotted as functions of the correlation time τ_c and compared to the corresponding fidelity obtained from the optimized GRAPE pulse sequence. The noise strength Δ is chosen to be $0.125 \times a_{\max}$ in this example. As expected, GRAPE yields the highest fidelities for all values of noise correlation time τ_c since it enforces optimization of the pulse sequence at every τ_c. Note that the fidelity curve of GRAPE has a global minimum. For this particular bit flip from the south to north pole of the Bloch sphere, the minimum lies near the correlation time $\tau_c \approx 3\hbar/a_{\max}$. The existence of a minimum is due to the fact that since the GRAPE pulse sequences are optimized for each value of τ_c, they will not only yield perfect unit fidelity in the zero-correlation time limit $\tau_c \to 0$, where GRAPE must reduce to the time optimal π pulse, but they will also yield unit fidelity in the long correlation time limit $\tau_c \to \infty$. The latter argument is true provided that the application of GRAPE does indeed find the global maximum of the fidelity, since small systematic errors can be corrected to arbitrary accuracy [34]. Consequently, there must be a minimum at a finite value of τ_c in the fidelity curve generated by GRAPE. The corresponding fidelity curves of the CORPSE and SCORPSE pulse sequences also show minima, reflecting the fact that these sequences also give unit fidelity in the limit $\tau_c \to 0$ and are specifically designed to correct to a high order the systematic errors in the limit $\tau_c \to \infty$. On the other hand, the fidelity curve for the π pulse is a monotonically decreasing function of the correlation time, reflecting the fact that this basic pulse does not provide any correction for systematic errors.

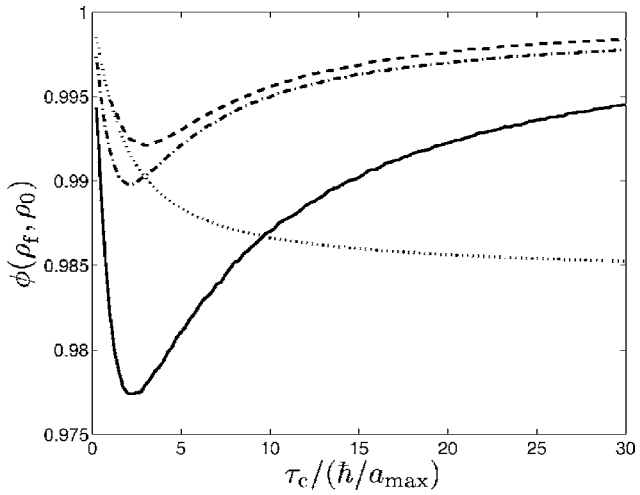

FIG. 1. Fidelities $\phi(\rho_f, \rho_0)$ for bit flip on computational basis states as functions of the noise correlation time τ_c, for a π pulse [Eq. (15), dotted line], CORPSE [Eq. (16), solid line], and SCORPSE [Eq. (17), dash-dotted line]. The optimized fidelity found using GRAPE is shown as the dashed line. The strength of the RTN in this example is $\Delta = 0.125 \times a_{\max}$.

Figure 1 also provides a good example of the general result that for intermediate noise correlation times, SCORPSE is more favorable than CORPSE. This is a consequence of the shorter operation time of SCORPSE than that of CORPSE, which appears to be more significant than the fact that CORPSE is more efficient than SCORPSE in correcting systematic errors. This balance between the length of the operation time and the accuracy in correcting systematic errors results

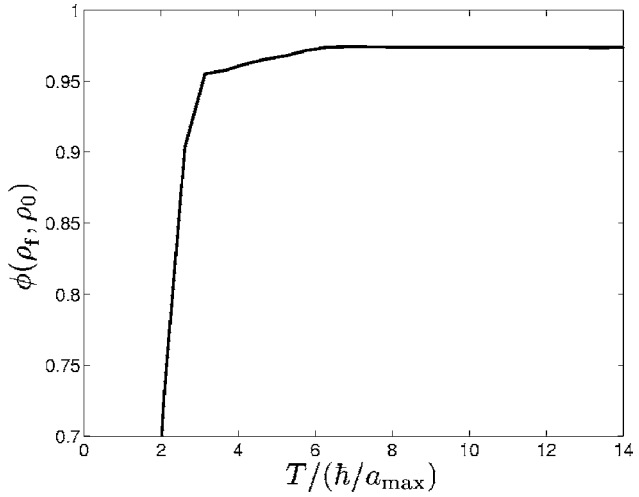

FIG. 2. Fidelity $\phi(\rho_f,\rho_0)$ of the GRAPE pulse sequence as a function of the operation time T, for noise correlation time $\tau_c = 5\hbar/a_{max}$ and noise strength $\Delta = 0.25 \times a_{max}$.

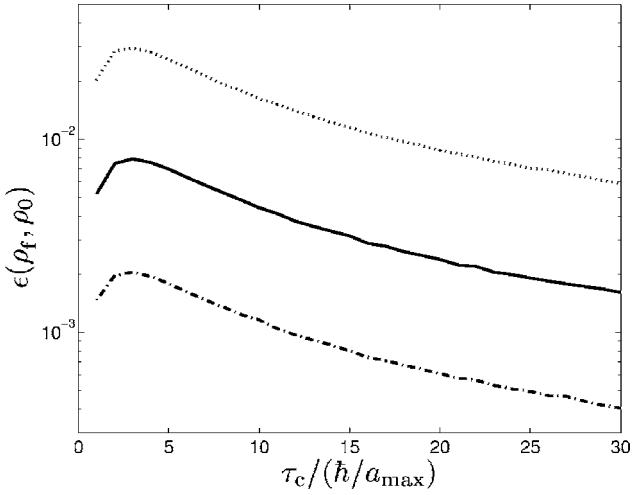

FIG. 3. Error $\epsilon(\rho_f,\rho_0) = 1 - \phi(\rho_f,\rho_0)$ of the GRAPE optimized pulse sequence, shown as a function of the correlation time τ_c for noise strengths $\Delta = 0.25 \times a_{max}$ (dotted line), $\Delta = 0.125 \times a_{max}$ (solid line), and $\Delta = 0.0625 \times a_{max}$ (dash-dotted line).

in a crossover between the fidelity curves of SCORPSE and CORPSE at very long correlation times, as required by the asymptotic fidelity expressions in Eqs. (19) and (20). This crossover occurs at larger values of τ_c than are shown in Fig. 1.

As discussed in Sec. III, the GRAPE algorithm for finding optimal pulse sequences involves optimization of the operation time T. However, the RTN used in this work does not have any dynamical effect on the initial density matrix ρ_0. Moreover, the probability of the noise amplitude to change its sign in any time interval of length δt does not depend on the earlier values of the noise amplitude and, hence, any pulse $a'(t)$ with operation time $T' < T$ may be extended to an operation time T without change of fidelity by setting

$$a(t) = \begin{cases} 0, & \text{for } 0 < t < T - T' \\ a'(t - T + T'), & \text{for } T - T' < t < T. \end{cases} \quad (27)$$

Thus, the fidelity is a monotonically increasing function of the operation time T. In fact, it is found that the fidelity saturates at a maximum value for rather short operation times, see, for example, Fig. 2.

Figure 3 shows the error $\epsilon(\rho_f,\rho_0) = 1 - \phi(\rho_f,\rho_0)$ of the GRAPE optimized result as a function of the correlation time τ_c, for several different noise strengths. A quadratic dependence of the error on the noise strength, $\epsilon \propto \Delta^2$, is observed over the parameter ranges $\Delta \in [a_{max}/16, a_{max}/4]$ and $\tau_c \in [0, 30\hbar/a_{max}]$.

B. One-qubit NOT gate

We now analyze the implementation of the one-qubit NOT gate under RTN, i.e., the bit flip state transformation for all initial states. The bit flip considered in Sec. IV A is a special case of the NOT gate, which is generally given as a π rotation about the x axis on the Bloch sphere. To assess the performance of the full quantum gate, we use the fidelity function Φ defined in Eq. (13) as a uniform average over pure initial states.

The π-pulse, CORPSE, and SCORPSE sequences are all specifically designed to implement a NOT gate and thus are the same here as in the previous section. However, the GRAPE pulse sequences for the bit flip on the computational basis states and for the full NOT gate differ, since the optimized fidelity functions are different for these two operations, compare Eqs. (11) and (13). Figure 4 shows the gate fidelities obtained with the π-pulse, CORPSE, SCORPSE, and GRAPE pulse sequences, as functions of the noise correlation time τ_c. The noise strength is chosen to be $\Delta = 0.125 \times a_{max}$, as in Fig. 1.

In comparison to the fidelities for the bit flip on computational basis states shown in Fig. 1, the fidelities for the NOT gate obtained with the CORPSE and SCORPSE pulse sequences are lower, whereas the fidelity obtained with the π pulse is

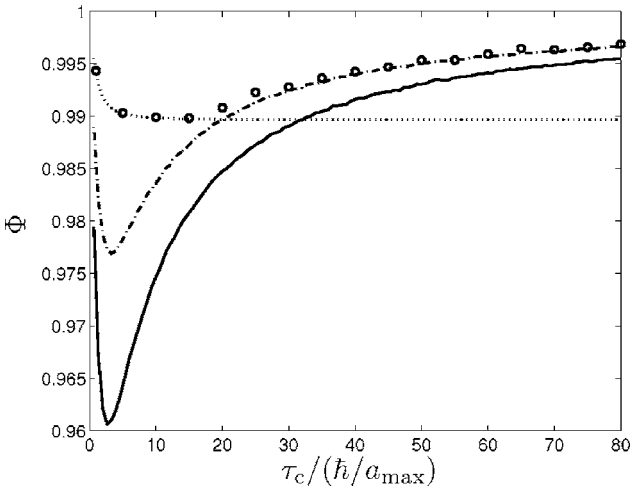

FIG. 4. Fidelities Φ for the NOT gate, shown as functions of the correlation time τ_c for a π pulse (dotted line), CORPSE (solid line), and SCORPSE (dash-dotted line). The figure also shows the optimized fidelity found using the GRAPE algorithm (circles). The RTN strength Δ is set at $0.125 \times a_{max}$.

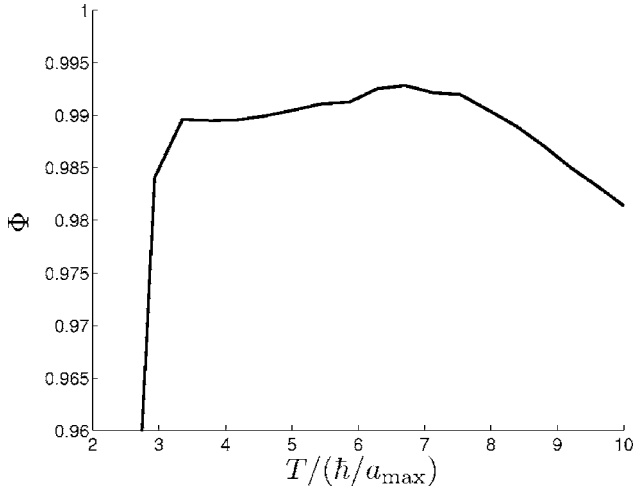

FIG. 5. Optimized fidelity Φ for the NOT gate obtained from GRAPE, shown as a function of the operation time T for noise correlation time $\tau_c = 30\hbar/a_{\max}$ and noise strength $\Delta = 0.125 \times a_{\max}$.

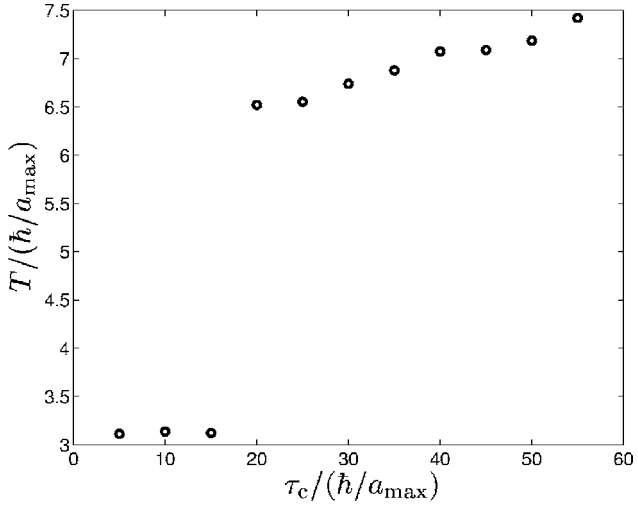

FIG. 6. Optimal operation time of pulse sequences obtained numerically with the GRAPE algorithm, shown as a function of the correlation time τ_c for noise strength $\Delta = 0.125 \times a_{\max}$.

higher. Nevertheless, Figs. 1 and 4 show, qualitatively, the same phenomena, namely, motional narrowing in the short correlation time limit $\tau_c \to 0$, where the π pulse is optimal, and the best correction of systematic errors at intermediate correlation times by the SCORPSE pulse sequence. In the long correlation time limit, there is again a crossover for the CORPSE sequence to yield the highest fidelity of these three pulse sequences.

Comparison of Figs. 4 and 1 show that the difference between the performance of GRAPE and the composite pulse sequences is less pronounced in the case of the NOT gate than for the bit flip on computational basis states. This observation is explained by the fact that the GRAPE algorithm searches a single pulse sequence, which is required to yield high fidelity for a large number of initial states for the NOT gate, whereas there is only one initial state in the bit flip on computational basis states. A remarkable aspect of Fig. 4 is that the GRAPE algorithm yields a fidelity very close to that of SCORPSE at values $\tau_c \gtrsim 30\hbar/a_{\max}$. However, this similarity in the fidelities does not imply a convergence of the GRAPE sequence to SCORPSE for any values of τ_c. Not only do the asymptotic limits for these two sequences differ as discussed above, but also the operation times are different, see below.

Since we employ the averaged gradient in Eq. (25), which requires the same amount of computation as three gradients for fixed initial conditions, one might conclude that finding the optimized pulse sequences for quantum gates will require approximately three times as much computational time as for the bit flip on the computational basis states. However, as noted above, the GRAPE algorithm finds the optimal operation time. This task is straightforward in the case of a bit flip on the computational basis states analyzed above, where the fidelity is a monotonically increasing function of the operation time. For the NOT gate, however, this optimization is nontrivial. In fact, because of the averaging over initial conditions, the optimal fidelity does not necessarily increase monotonically with T, as is illustrated in Fig. 5. Finding the optimal operation time for a quantum gate independent of the initial conditions, thus, clearly increases the complexity of the problem.

Additional insight into the efficiency of the GRAPE pulse sequence may be obtained by examining the behavior of the optimal operation time as a function of the correlation time. As shown in Fig. 6, the optimal operation time of GRAPE increases sharply to values close to the operation time of the SCORPSE pulse sequence at a value $\tilde{\tau}_c \approx 18\hbar/a_{\max}$. For longer correlation times than $\tilde{\tau}_c$, the fidelity obtained with GRAPE is only marginally above that obtained with SCORPSE, see Fig. 4. It appears from Fig. 4 that errors due to RTN cannot be efficiently corrected with bounded controls for correlation times shorter than $\tilde{\tau}_c$, and therefore, the optimal operation time of GRAPE reduces to that of a π pulse in this regime.

V. SUMMARY AND CONCLUSIONS

In this work, we have shown how to perform high-fidelity quantum operations using bounded control fields on a one-qubit system that is subject to random telegraph noise acting on the qubit energy splitting. We considered examples of two types of quantum operations, namely, a state transformation and a quantum gate. For the state transformation, we chose a bit flip on the computational basis states, in which the one-qubit state is flipped from the south pole of the Bloch sphere to the north pole. As the quantum gate, we used the one-qubit NOT gate, which generates a complete π rotation on the Bloch sphere about the x axis independent of the initial state of the system.

In both cases, we compared the fidelities obtained from the π pulse to the fidelities obtained from the CORPSE and SCORPSE composite pulse sequences. In the limit of vanishing noise correlation time τ_c, motional narrowing occurs. This effect renders the π pulse to be the most accurate sequence since it is time optimal in implementing a bit flip on almost all states. On the other hand, the CORPSE sequence yields the highest fidelity in the long correlation time limit $\tau_c \to \infty$, since it is designed to be the most accurate three-pulse sequence for correction of systematic errors. Over a rather wide intermediate range of values of correlation time

τ_c, it is found that SCORPSE yields the highest fidelity among the three standard pulse sequences, suggesting that this may be a useful approach to suppress environmental noise in physical realizations of quantum computers.

We also calculated pulse sequences numerically to optimize the fidelities, using a modification of the gradient ascent pulse engineering method and compared the results of this numerical approach to the standard composite pulse sequences. The combination of the original GRAPE algorithm with a unitary quantum trajectory approach that is implemented here provides an adaptive way of generating pulse sequences that optimizes gate and state transformation fidelities in the presence of noise. One key feature that emerges from this work is that the fidelity optimized pulse sequences obtained using the GRAPE algorithm were always found to yield higher fidelities than the most accurate composite pulse sequence. Furthermore, our method is applicable to noise with arbitrary correlation time, allowing generation of decoherence suppressing pulse sequences in all dynamic regimes of noise. This property is particularly useful in the intermediate regime where neither dynamical decoupling nor control methods based on Markovian master-equation descriptions can be used.

In this work, we employed an unbiased average over initial states to obtain the fidelity measure Φ for a quantum gate. A useful extension of this approach would be to combine the same methodology with an optimization of the quantum state fidelity function $\phi(\rho_f, \rho_0)$ to locate its minimum with respect to the initial state. Although involving a considerably greater numerical effort, this could be particularly useful for determination of more specific lower bounds on the gate fidelity.

The results of this paper provide useful average bounds for the implementation of high-fidelity one-qubit operations in a noisy system without ancillary qubits. Although a simple RTN noise model is used in this paper, we expect that the qualitative dependency of the fidelity on noise strength and correlation time will also be present in a general qubit-bath system. In particular, it will be of interest to apply the methods presented here to the study of different noise models, e.g., Gaussian noise with a $1/f$ spectrum and noise in both σ_z and σ_x directions in the Hamiltonian of Eq. (1). Other possible extensions of this work include high-fidelity control of multiqubit systems. Recent work has addressed optimal control of noiseless coupled superconducting qubits [35]. For these systems, the environmental noise may act on each qubit in either a correlated or uncorrelated fashion, introducing additional noise variables. These may be treated in exactly the same way as done here, without any formal modification. Coupling qubits will introduce entanglement and require that the density-matrix dynamics be analyzed for a higher-dimensional system. There do not appear to be any formal limitations to extending the analysis to this expanded set of questions for noisy multiqubit systems, although a reformulation of the equations for the fidelity and its gradient will be required. One important open issue that would be addressable by this approach is to find a control sequence for the interqubit coupling term that implements a controlled NOT gate with high fidelity in the presence of noise.

ACKNOWLEDGMENTS

We thank the NSF for financial support under ITR Grant No. EIA-0205641, and DARPA and ONR under Grant No. FDN0014-01-1-0826 of the DARPA SPINs program. M. M acknowledges the Academy of Finland, the Finnish Cultural Foundation, and Jenny and Antti Wihuri Foundation for financial support. We would like to express our appreciation to S. J. Glaser and V. Shende for helpful discussions.

[1] P. W. Shor, Phys. Rev. A **52**, R2493 (1995).
[2] A. M. Steane, Phys. Rev. Lett. **77**, 793 (1996).
[3] P. Zanardi and M. Rasetti, Phys. Rev. Lett. **79**, 3306 (1997).
[4] D. A. Lidar, I. L. Chuang, and K. B. Whaley, Phys. Rev. Lett. **81**, 2594 (1998).
[5] E. Knill, R. Laflamme, and L. Viola, Phys. Rev. Lett. **84**, 2525 (2000).
[6] L. Viola and S. Lloyd, Phys. Rev. A **58**, 2733 (1998).
[7] L. Viola, S. Lloyd, and E. Knill, Phys. Rev. Lett. **83**, 4888 (1999).
[8] L. Viola and E. Knill, Phys. Rev. Lett. **90**, 037901 (2003).
[9] H. M. Wiseman, Phys. Rev. A **49**, 2133 (1994).
[10] H. M. Wiseman, Phys. Rev. A **50**, 4428.2 (1994).
[11] H. Rabitz, R. de Vivie-Riedle, M. Motzkus, and K. Kompa, Science **288**, 824 (2000).
[12] J. F. Poyatos, J. I. Cirac, and P. Zoller, Phys. Rev. Lett. **77**, 4728 (1996).
[13] M. A. Pravia, N. Boulant, J. Emerson, A. Farid, E. M. Fortunato, T. F. Havel, R. Martinez, and D. G. Cory, J. Chem. Phys. **119**, 9993 (2003).
[14] N. Khaneja, B. Luy, and S. J. Glaser, Proc. Natl. Acad. Sci. U.S.A. **100**, 13162 (2003).
[15] T. D. Ladd, D. Maryenko, Y. Yamamoto, E. Abe, and K. M. Itoh, Phys. Rev. B **71**, 014401 (2005).
[16] Y. Nakamura, Y. A. Pashkin, T. Yamamoto, and J. S. Tsai, Phys. Rev. Lett. **88**, 047901 (2002).
[17] E. Collin, G. Ithier, A. Aassime, P. Joyez, D. Vion, and D. Esteve, Phys. Rev. Lett. **93**, 157005 (2004).
[18] N. G. van Kampen, *Stochastic Processes in Physics and Chemistry* (Elsevier, Amsterdam, 1992).
[19] E. Paladino, L. Faoro, G. Falci, and R. Fazio, Phys. Rev. Lett. **88**, 228304 (2002).
[20] Y. M. Galperin, B. L. Altshuler, and D. V. Shantsev, e-print cond-mat/0312490.
[21] R. de Sousa, K. B. Whaley, F. K. Wilhelm, and J. von Delft, Phys. Rev. Lett. **95**, 247006 (2005).
[22] S. Kogan, *Electronic Noise and Fluctuations in Solids* (Cambridge University Press, Cambridge, England, 1996).
[23] T. Fujisawa and Y. Hirayama, Appl. Phys. Lett. **77**, 543 (2000).
[24] C. Kurdak, C.-J. Chen, D. C. Tsui, S. Parihar, S. Lyon, and G. W. Weimann, Phys. Rev. B **56**, 9813 (1997).

[25] K. R. Brown, A. W. Harrow, and I. L. Chuang, Phys. Rev. A **70**, 052318 (2004).
[26] J. J. L. Morton, A. M. Tyryshkin, A. Ardavan, K. Porfyrakis, S. A. Lyon, and G. A. Briggs, Phys. Rev. A **71**, 012332 (2005).
[27] L. M. K. Vandersypen and I. L. Chuang, Rev. Mod. Phys. **76**, 1037 (2004).
[28] H. K. Cummins and J. A. Jones, New J. Phys. **2**, 1 (2000).
[29] H. K. Cummins, G. Llewellyn, and J. A. Jones, Phys. Rev. A **67**, 042308 (2003).
[30] K. Blum, *Density Matrix Theory and Applications* (Plenum Press, New York, 1996).
[31] N. Khaneja, T. Reiss, C. Kehlet, T. Schulte-Herbrüggen, and S. J. Glaser, J. Magn. Reson. **172**, 296 (2005).
[32] M. A. Nielsen and I. L. Chuang, *Quantum Computation and Quantum Information* (Cambridge University Press, Cambridge, England, 2000).
[33] C. P. Slichter, *Principles of Magnetic Resonance* (Springer-Verlag, Berlin, 1996).
[34] H. Geen and R. Freeman, J. Magn. Reson. **93**, 93 (1991).
[35] A. K. Spoerl, T. Schulte-Herbrueggen, S. J. Glaser, V. Bergholm, M. J. Storcz, J. Ferber, and F. K. Wilhelm, quant-ph/0504202 (unpublished).